Biosorption of Pb^{2+} by original and protonated citrus peels: Equilibrium, kinetics, and mechanism

Silke Schiewer *, Ankit Balaria [1]

Department of Civil & Environmental Engineering, University of Alaska Fairbanks, PO Box 755900, Fairbanks, AK 99775, USA

ABSTRACT

Biosorption can be an efficient low-cost process to remove toxic heavy metals from wastewater. This study investigated the uptake of Pb^{2+} by processed orange peels, a pectin-rich byproduct of the fruit juice industry. Potentiometric titrations showed a significantly higher negative surface charge of protonated peels compared to original peels, with acidic groups around pH 4, 6, and 10. FTIR spectra of peels were similar to those of pectin. The carboxylic group peak shifted from 1636 to 1645 cm^{-1} after Pb^{2+} binding, indicated the involvement of carboxyl groups in Pb^2 binding. Depending on the particle size, equilibrium was achieved in 30 min to 2 h. The first-order model was inferior to second- or third-order models. The obtained rate constants were much higher for smaller particles, while the capacity was similar for all sizes. Low pH, increased ionic strength, or competing co-ions reduced Pb^{2+} binding at low sorbent dosages, but at high sorbent dosages removal remained above 90%. The Pb^{2+} uptake at 300 ppm was 2 mmol/g (40% of the dry weight). Due to high uptake, favorable kinetics and good stability, citrus peel biosorbents hold high promise for industrial applications.

© 2008 Elsevier B.V. All rights reserved.

1. Introduction

Pollution of surface waters by toxic heavy metals such as Pb from industrial sources and storm water runoff is an important environmental problem. To treat large volumes of waste streams, for example from mining operations, cost-efficient processes are required. Biosorption is a promising technique for this purpose [1], especially if low-cost biosorbents based on byproducts of other industries are used.

1.1. Sorbent selection

The effectiveness of biosorbents depends to a large extent on their biochemical composition, particularly on functional groups available in cell wall polysaccharides. Carboxyl groups can play an important role in metal biosorption by algal biosorbents [2]. Pectin, a cell wall polysaccharide of higher plants, is based mainly on galacturonic acid, features a large number of carboxyl groups, and has a known ability to bind divalent cations [3,4]. Therefore, pectin-rich materials such as citrus peels, from

which pectin is commercially extracted, have a high potential for metal binding. A number of pectin-rich byproducts have been studied for their metal-binding abilities including apple waste [5,6], sugar beet pulp [7–9], orange peels [10–14], orange and banana peels [15], citrus peels and coffee husks [16], and different fruit materials, such as several types of citrus peel [17]. In the present work, a processed citrus peel product was utilized for biosorption of Pb^{2+} because of the high pectin content of citrus peels.

1.2. Characterization of sorbent functional groups

Potentiometric titration can be used to evaluate the charge of sorbent particles at different pH values based on the electroneutrality equation of the solution [18]. This method has been used to characterize pK_a values of the functional groups present in biosorbents such as brown seaweeds [19], sugar beet pulp [9], and protonated pectin peels from fruit juice production [20]. To complement information from potentiometric titrations, Fourier transform infrared (FTIR) spectroscopy can be used to characterize the functional groups of biomaterials, as done for different kinds of pectin [21–23]. In contrast to compounds such as pectin or oils extracted from peels, very little FTIR research has been reported for whole citrus peels. Perez-Marin et al. [13] characterized orange peels by FTIR, however the interpretation was vague and inconclusive.

* Corresponding author. Tel.: +1 907 474 2620; fax: +1 907 474 6087.
  E-mail address: ffsos@uaf.edu (S. Schiewer).
[1] Present address: 151 Link Hall, Civil and Environmental Engineering, Syracuse University, Syracuse, NY 13244, USA.

1.3. Kinetic studies

Though a variety of models can be applied to describe biosorption kinetics [24], those most commonly used are pseudo-first-order and pseudo-second-order models. Ajmal et al. [10] studied kinetics of Ni sorption by orange peels and modeled the rate using first-order kinetics with maximum sorption achieved in approximately 2 h. Without comparing different models, Li et al. [12] and Xuan et al. [25] concluded that a first-order model fit for Cd and Pb sorption, respectively, to chemically modified orange peels. Reddad et al. [9] found that a second-order rate model fits well for kinetics of Ni^{2+} and Cu^{2+} biosorption by pectin-rich sugar beet pulp. Schiewer and Patil [17] determined that a second-order model fit better than a first-order model for biosorption of Cd^{2+} by protonated pectin peels. Perez-Marin et al. [13] compared a pseudo-first-order model, a pseudo-second-order model, the Elovich equation [26], and a simple expression for intraparticle diffusion, and found the Elovich equation best described Cd sorption by orange peels. The contradictory results found in the literature necessitate further study of suitable kinetic models for biosorption by citrus peels. Furthermore, studies on biosorption kinetics of citrus peels or related materials have so far been confined to simple first- and second-order kinetic models. Other rate expressions should be taken into consideration.

1.4. Effects of environmental conditions

Biosorption of metal ions depends on parameters such as pH, temperature, ionic strength, metal concentration, co-ion presence, and sorbent properties. Annadurai et al. [15] found that uptake of Pb^{2+}, Ni^{2+}, Zn^{2+}, Cu^{2+}, and Co^{2+} increases with pH due to competition of metal ions with protons at lower pH values. Lee and Yang [5] determined that Cu^{2+} binding by pectin-rich apple waste was highest at pH 5.5–7.5. Cu sorption was only slightly affected by ionic strength up to 0.1N, but decreased at higher ionic strength or in the presence of competing co-ions Ni^{2+} and especially Pb^{2+}. Apparently monovalent ions have little impact on metal binding, whereas more strongly bound divalent competing ions can reduce binding of the target metal. Pb is often one of the most strongly bound ions in biosorption. Therefore, the question arises whether Pb biosorption by citrus peels is similarly affected by these parameters.

1.5. Biosorption isotherms

Biosorption isotherms are useful in quantitatively evaluating and predicting the process performance of the binding capacity and affinity for different metal concentrations and sorbent dosages. The Langmuir and Freundlich isotherms are most commonly used due to their simplicity and ease of interpretation. Annadurai et al. [15] found that the Freundlich model fit better than the Langmuir model for biosorption of Cu^{2+}, Co^{2+}, Ni^{2+}, Zn^{2+}, and Pb^{2+} on banana and orange peels. Jumle et al. [16] were also able to fit the sorption of Hg^{2+}, Pb^{2+}, and Zn^{2+} ions by citrus peels and coffee husks using the Freundlich isotherm model. Schiewer and Patil [17] found similarly good fits of Langmuir and Freundlich isotherms for Cd binding by lemon, orange, and grapefruit peels at pH 3 and pH 5; some isotherm data at pH 5, however, did not match either model. Using the Langmuir isotherm, Reddad et al. [9] modeled biosorption of Ni^{2+} and Cu^{2+} ions on sugar beet pulp and obtained a good fit of the data. Perez-Marin et al. [13] found that the Sips isotherm fit best for Cd sorption by orange peels, followed by Redlich-Peterson, Langmuir, and Freundlich isotherms. It is not surprising that the Sips model fit best since it has an additional fitting parameter compared to the Langmuir model, which it otherwise resembles.

1.6. Objectives

The objectives of this research were to characterize the surface charge and functional groups involved in metal binding of citrus peel sorbents by potentiometric titrations and FTIR spectroscopy. Different kinetic models were compared for their ability to describe Pb^{2+} binding by citrus peels. The effect of environmental conditions such as pH, co-ions, and ionic strength on overall binding by citrus peels was studied, and the effect of metal concentration was described by sorption isotherms. Further information about the binding mechanism was obtained from changes in pH during incremental addition of Pb^{2+} to citrus peel suspensions.

2. Materials and methods

2.1. Materials

Dried and ground processed orange peels (Valencia) were supplied by Robert Jones of Alarma Consulting Corporation in Florida. These peels were sieved into different size fractions. For most experiments, original untreated peels were used; however, pH titrations and FTIR studies were also performed with protonated peels. Protonation was carried out by suspending the sorbent material in 0.1 M HNO_3 (10 g of peels/L) for 3 h, rinsing with double-deionized water, and drying for 12 h at 40 °C, in order to remove naturally present ions (e.g., Ca^{2+}) from the orange peels. There was no significant weight loss during protonation.

All experiments were conducted using double-deionized water and ACS reagent-grade chemicals. Nitrate salt of Pb^{2+} was used for metal-binding experiments to avoid complex formation with ligands in solution. Nitric acid and sodium hydroxide were used for pH adjustment, and sodium nitrate was used for adjusting the ionic strength of the solution.

2.2. Potentiometric titrations

Potentiometric titrations were performed in a closed system (N_2-atmosphere) in order to avoid interference from atmospheric CO_2. An amount of 0.2 g sorbent was suspended in 200 ml double-deionized water with a background electrolyte concentration of 0.01 M $NaNO_3$. After the initial pH became constant, known amounts of NaOH were incrementally added, and pH values of the solution were measured until pH 10 was reached. The surface charge (S) on the peel particle with mass (m) was calculated according to Eq. (1) based on the electroneutrality equation of the solution with volume (V):

$$[S] = ([OH^-] + [NO_3^-] - [H^+] - [Na^+])V/m \quad (mequiv./g) \qquad (1)$$

Since NO_3^- and Na^+ from the background electrolyte cancel each other's charge, only the equivalents of NO_3^- from acid addition and Na^+ from base addition have to be considered in addition to OH^- and H^+ from pH measurements.

2.3. FTIR experiments

Citrus peels were characterized with respect to their surface functional groups using FTIR spectroscopy. FTIR was also used to identify functional groups responsible for binding Pb^{2+}. Original dry peels or Pb^{2+}-loaded peels (filtered and dried after contact with an initial Pb^{2+} concentration of 0.1 mM at pH 5) were mixed with KBr at a ratio of 1:100 and compressed into films for FTIR analysis using a Thermo Scientific Nicolet IR100 spectrometer. Infrared (IR) absorbance data were obtained for wave numbers 400–4000 cm^{-1}.

IR data were collected, processed, and analyzed using the software Encompass^{TM} (Copyright$^©$ 2003 by Thermo Electron Corporation).

2.4. Lead-binding experiments: general conditions

Biosorption experiments were conducted in an open system to simulate practical environmental application. Visual Minteq modeling confirmed that no precipitation of $PbCO_3$ occurred, and the $Pb(HCO_3)^+$ concentration was negligible (0.028%) for the given environmental conditions. Experiments were conducted in acid-washed 200-ml Nalgene reactor bottles with continuous stirring using a magnetic stirrer. Standard conditions for experiments were as follows: Pb concentration 0.1 mM (20.7 ppm); peel size 0.6–1 mm; peels concentration 0.1 g/L; 200 mL solution; pH 5; background electrolyte concentration 0.01 M $NaNO_3$; room temperature 21–25 °C. Samples were filtered using a 0.2-μm membrane filter, and the Pb concentration of the filtrate was analyzed using Graphite Atomic Absorption spectrometry (PerkinElmer AAnalyst 300).

2.5. Kinetic experiments

Kinetic experiments were conducted in order to determine the equilibration time and binding rate of Pb^{2+} binding by citrus peels. The effect of sorbent size on sorption kinetics was investigated, following the above described methodology, using orange peels of different sizes: smaller than 0.6, 0.6–1, and 1–3 mm. Sampling times ranged from as low as 2 min to as high as 3 h, based on preliminary experiments. Five-milliliter samples were taken periodically using a syringe and filtered using 0.2-μm membrane filters. Data were modeled using both first- and second-order kinetic models. The pseudo-first-order model (model a) assumes that the rate of change of surface site concentration is proportional to the amount of remaining unoccupied surface sites:

$$\frac{dq}{dt} = k_a(q_e - q) \tag{2}$$

where q and q_e are adsorbed amounts (mg/g) at time (t) (min) and equilibrium, respectively, and k_1 (min^{-1}) is the first-order Lagergren adsorption rate constant [27]. This model can be linearized as

$$\log(q_e - q) = \log q_e - \frac{k_a}{2.303}t \tag{3}$$

The pseudo-second-order model (model b) assumes that the rate is proportional to the square of the number of remaining free surface sites [28]:

$$\frac{dq}{dt} = k_b(q_e - q)^2 \tag{4}$$

with the second-order adsorption rate constant (k_b) (g/mequiv.-min). This model can be linearized as

$$\frac{t}{q} = \frac{1}{k_b q_e^2} + \frac{t}{q_e} \tag{5}$$

We also considered an overall second-order model where that the rate is proportional to the metal concentration in solution and the number of remaining free surface sites at any time t (model c):

$$\frac{dq}{dt} = k_c C(q_e - q) \tag{6}$$

Finally, an overall third-order model was considered where that the rate is proportional to the metal concentration in solution and the square of the number of remaining free surface sites (model d):

$$\frac{dq}{dt} = k_d C(q_e - q)^2 \tag{7}$$

The parameters k and q_e for all models were determined by nonlinear parameter optimization, minimizing the root mean square error (RMSE) using the Solver function in Excel. In addition, parameters for models a and b were also derived from linearizations. For models c and d, an explicit integrated equation cannot easily be obtained since C changes with time. Therefore, these equations were numerically integrated in Excel.

2.6. Effect of environmental conditions

Effects of important environmental conditions were investigated for sorbent dosages of 0.1 and 1.0 g/L, providing limited and excess sites, respectively, at a Pb^{2+} concentration of 0.1 mM under equilibrium conditions. Three pH values (3, 4, and 5) were investigated, and the presence of divalent metal ions Ca^{2+} and Ni^{2+}, each added individually, was studied at equimolar concentrations (0.1 mM). Background electrolyte concentrations were 0, 10^{-2}, and 10^{-1} M $NaNO_3$.

2.7. Isotherms

Isotherms were obtained by varying the initial metal ion concentration from 20 to 400 mg/L (9.65×10^{-2} to 1.93 mM). An equilibration time of 3 h was allowed. Equilibrium sorption was modeled using the Langmuir and the Freundlich isotherms because of their ease of interpretation. The Langmuir model considers that the sorbent surface contains only one type of binding site and sorption of one ion per binding site is taking place. This can be described as

$$q_e = \frac{K q_{max} C_e}{1 + K C_e} \tag{8}$$

where q_e is the metal uptake, q_{max} is the maximum biosorption capacity, K is a constant related to adsorption energy, and C_e is the equilibrium concentration of metal ions. The Langmuir parameters can be determined from the slope and intercept when plotting C_e/q_e versus C_e, based on a linearized form of Eq. (8) and written as

$$\frac{C_e}{q_e} = \frac{1}{K q_{max}} + \frac{C_e}{q_{max}} \tag{9}$$

The empirical Freundlich model considers no surface saturation and can be expressed as

$$q_e = k_f C_e^{1/n} \tag{10}$$

where k_f and n are model constants that can be determined from the slope and intercept when $\log q_e$ is plotted versus $\log C_e$, according to the linearized form of Eq. (10):

$$\log q_e = \log k_f + 1/n \log C_e \tag{11}$$

2.8. Modeling error analysis

In order to evaluate the error of the model predictions, the root mean square errors (RMSE) were calculated for kinetic and isotherm models. The sum of the square of the difference between metal removal experimental data (q), and model predictions (q_m) was divided by the number of data points (p) for each data set, and the square root of this term was taken:

$$RMSE = \sqrt{\frac{\sum_1^p (q - q_m)^2}{p}} \tag{12}$$

For kinetic models and isotherms, nonlinear parameter optimization was performed by varying the model parameters while minimizing the RMSE value in order to obtain a better fit of the experimental data than is achieved by linearizations.

3. Results and discussion

3.1. Characterization of sorbent charge by potentiometric titration

Potentiometric titrations were conducted in order to determine the overall negative charge of the sorbent, since electrostatic attraction between negatively charged sorbents and positively charged metal ions could be a relevant binding mechanism. Fig. 1 represents the total negative surface charge of protonated and original orange peels for a background electrolyte concentration of 0.01 M NaNO$_3$. It can be observed that protonated peels have a much higher negative charge than unprotonated peels, which only develop a significant charge at alkaline pH. Protonation removes cations such as Ca^{2+} that are bound to the original peels, replacing them with protons. The protonated peels, therefore, have a negative surface charge when the pH exceeds the pK_a of the peels' functional groups, whereas calcium binding to functional groups neutralizes the charge of original peels. The original peels become charged at higher pH when additional groups not saturated with calcium are deprotonated. Protonated pectin peels can show higher metal-binding capacity and affinity than unprotonated peels, as observed by Schiewer and Patil [20] for Cd biosorption. This may be due to the fact that protonation increases the negative charge which facilitates electrostatic attraction of metal cations and removes competing cations.

The titration curve for protonated peels shows a rapid decline around pH 4, 6 and 10. This suggests that there are functional groups present around these pH values which buffer the solution. These groups may be carboxyl groups (pK_a ∼3 to 5) and hydroxyl groups (pK_a ∼10) [29]. Due to difficulties in determining the surface charge accurately at very low and very high pH values, where S is very sensitive to minute variations in pH (Eq. (1)), the titration curve could not be extended beyond the range 4–10. The observed values are similar to pK_a values 3.8, 6.4, 8.4, and 10.7, determined with the help of a continuous pK_a spectrum for lemon-based protonated pectin peels [20].

The sharp charge decline at pH 4 and 10 corresponds to that observed by Balaria and Schiewer [21] for citrus pectin. At pH 5, where carboxyl groups are mostly deprotonated, the surface charge was −0.7 mequiv./g for pectin with a low degree of methoxylation (9%) and −0.3 mequiv./g for pectin with a high degree of methoxylation (64%) [21] compared to −0.33 mequiv./g for protonated and −0.01 mequiv./g for original peels, as determined in the present study at the same background electrolyte concentration of 0.01 M NaNO$_3$. Since methoxylation consumes carboxyl groups, the low-

methoxylated (LM) pectin should have 2.5 (91%/36%) times as many available unmethoxylated carboxyl groups as high-methoxylated (HM) pectin. That is consistent with the charge of LM pectin being about 2.3 (0.7/0.3) times as high as for HM pectin. Citrus peels typically have a pectin content of about 20–30%, and generally, citrus pectin has a low degree of acetylation [7]. Consequently, it can be expected that the charge of citrus peels is about 30% of that for LM pectin, which would be −0.2 mequiv./g. The processed citrus peel used in this study shows a somewhat higher charge of −0.33 mequiv./g at pH 5. That can be explained by a higher pectin content since some other compounds had already been removed from the peel. Therefore, the comparative magnitudes of charge for these materials are reasonable. The results show that the charges observed at pH 5 are consistent with those expected based on the carboxyl groups known to be present in pectin. This means that at pH 5, other possible acidic groups likely play only a minor role.

3.2. FTIR characterization of functional groups and their contribution to metal binding

FTIR results revealed that pectins (Fig. 2a and b, data from [21]) and peels (Fig. 2c–g) have very similar spectra, which confirmed that pectin is an important component of orange peels and has similar functional groups. All spectra have a hydroxyl (−OH) peak at wave number ∼3440 cm^{-1}, alkyl (−CH$_n$) peak at wave number ∼2920 to 2935 cm^{-1}, a peak at wave number ∼1740 to 1750 cm^{-1} for the C=O bond of carboxyl groups and their esters, and another peak at wave number ∼1625 to 1645 cm^{-1} for asymmetric stretching of the carboxylic C=O double bond. A peak around 1382 cm^{-1} was observed both for protonated and metal laden peels (Fig. 2c–f) but not for pectin or original peels without Pb. This peak has been attributed to the C−O bond in carboxyl groups of alginic acid that had bound heavy metals [31]. The earlier parts of the spectra (i.e., wave numbers 1000–1500 cm^{-1}) are also quite similar in all the sorbent materials. This part represents various configurations of C, O, N, and H bonds in the pectin and peel structures [22,23].

The peak around 1382 cm^{-1} (Fig. 2c–f), which was not observed for original peels or pectins, was probably due to new bond formation between Pb^{2+} and carboxyl groups [31]. This is plausible because a large similar new peak was observed for Pb-laden LM pectin and a lower peak for Pb-laden HM pectin whereas no such peak had been observed for pectin without exposure to metal ions [21]. The size of that peak did however not change significantly with metal concentration (Fig. 2e–f).

No strong shift in the carboxyl peak with wave numbers around 1740 was observed in either case (Fig. 2c–g). However, the carboxylic group absorption peak around 1640 shifted significantly for protonated peels from 1636 to 1645 cm^{-1} after metal binding (Fig. 2c and d). A similarly strong shift was observed for HM pectin [21]. The shift in wave number corresponds to a change in energy of the functional group, indicating that the bonding pattern of carboxyl groups changes after sorption. This result confirmed the involvement of carboxyl groups in binding of Pb^{2+} for pectin and protonated peels. The shift of the (−COOH) peak was not strong in original orange peels (1635 cm^{-1} compared to 1638 cm^{-1}, Fig. 2e–g). This may be because these groups were already at a similar energy level due to naturally present Ca^{2+} bound to the carboxylic acid groups, which were later replaced by Pb^{2+} ions. Similar peaks were observed for seaweed and their component alginic acid, where the peak around 1640 cm^{-1} was attributed to metal chelates of carboxyl groups [30–33]. The comparison of the peel spectra with the pectin spectra lead to the conclusion that carboxylic acid groups of pectin were likely responsible for binding Pb^{2+} by orange peels.
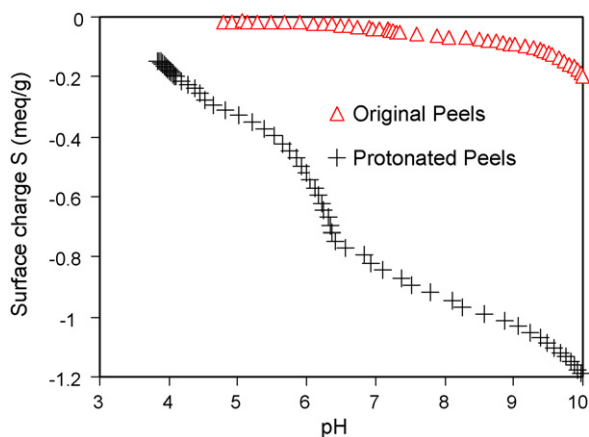

Fig. 1. Potentiometric titrations of untreated and protonated orange peels at a background electrolyte concentration of 0.01 M NaNO$_3$.
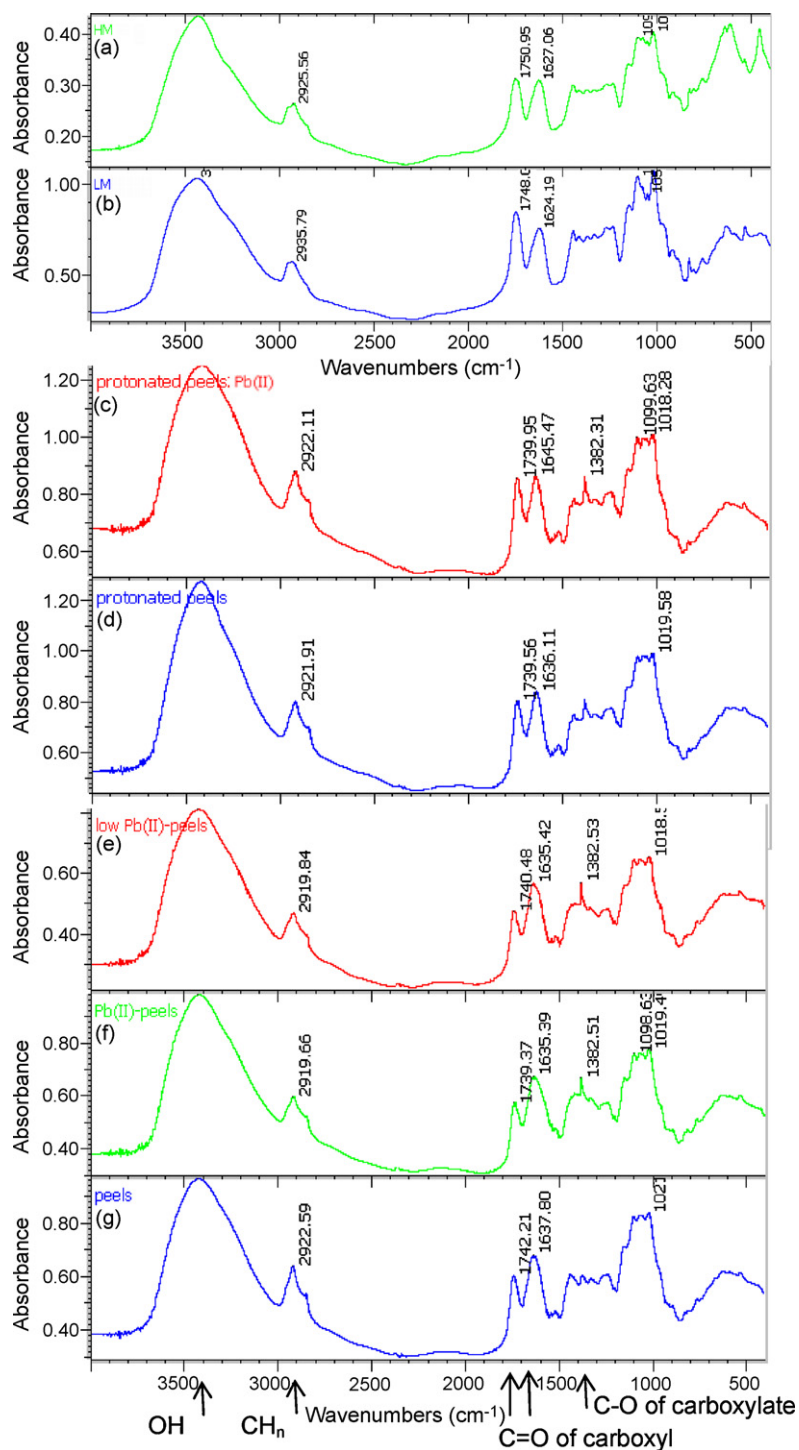
Fig. 2. FTIR spectra of (a) HM pectin, (b) LM pectin, (c) protonated peels with 0.1 mM Pb^{2+}, (d) protonated peels without Pb^{2+}, (e) original peels at 0.01 mM Pb^{2+} (low Pb(II)-peels), (f) original peels at 0.1 mM Pb^{2+} (Pb(II)-peels), and (g) original peels without Pb.

3.3. Batch kinetics

Kinetic studies are not only necessary to determine the equilibration time for biosorption but also important for designing treatment systems based on the reaction rate. Fig. 3 presents data for binding of Pb^{2+} by orange peels of three different sizes: smaller than 0.6, 0.6–1, and 1–3 mm. The smallest peels reached equilibrium within the first 30 min, whereas the larger sizes took about 1–2 h to attain equilibrium. Equilibrium metal removal

was 80–90% for smaller sizes and 70–80% for the largest size (1–3 mm).

Kinetic models with different reaction orders were used and nonlinear fitting was performed to determine the model parameters (binding rate constant and equilibrium uptake). Table 1 summarizes the rate constants (k) and equilibrium uptake (q_e) determined by nonlinear parameter optimization for the three sizes of peels according to different models as well as those obtained from linearizing the second-order model (Eq. (5)).

Table 1
Kinetic parameters for Pb^{2+} biosorption by orange peels for different models

	<0.6 mm			0.6–1 mm			1–3 mm			Average
	k	q_e (mmol/g)	RMSE (mmol/g)	k	q_e (mmol/g)	RMSE (mmol/g)	k	q_e (mmol/g)	RMSE (mmol/g)	RMSE (mmol/g)
Model a	0.47	0.84	0.043	0.33	0.83	0.058	0.25	0.71	0.065	0.055
Model b	0.86	0.87	0.021	0.48	0.85	0.034	0.21	0.77	0.039	0.031
Model b[a]	0.67	0.88	0.023	0.29	0.90	0.051	0.14	0.78	0.044	0.039
Model c	5.95	0.87	0.019	4.17	0.86	0.030	2.86	0.73	0.045	0.031
Model d	7.35	0.90	0.018	5.13	0.97	0.029	4.49	0.81	0.024	0.023

(a) First-order model: rate proportional to number of free sites, $r = k(q_e - q)$. (b) Second-order model: rate proportional to square of number of free sites, $r = k(q_e - q)^2$. (c) Second-order model: rate proportional to Pb^{2+} concentration and number of free sites, $r = kC(q_e - q)$. (d) Third-order model: rate proportional to Pb^{2+} concentration and square of number of free sites, $r = kC(q_e - q)^2$.

[a] Parameters from linearization.

When parameters were determined from linearizations (Eqs. (3) and (5)), R^2 values for the first-order model were very low (0.5–0.76), resulting in a bad fit. For the second-order model, significantly lower k values were obtained (22–40% lower than for nonlinear fitting) and RMSE were in average 25% higher (9.5%, 50% and 12.8%, respectively, for the different sizes) than for nonlinear parameter optimization in spite of R^2 values of 0.999. Nonlinear fitting, therefore, should be used even if linearizations yield excellent R^2 values.

Both rate constant and equilibrium uptake were found to be dependent on the size, being higher for smaller sizes. The smallest particles (<0.6 mm) had a significantly higher rate constant than peels of larger sizes, which indicates that the sorption rate is affected by mass transfer. The equilibrium uptake for the two smaller sizes was almost equal and slightly higher than that for the peels of 1.0–3.0 mm in spite of much larger external surface area for small particles. The similar equilibrium uptake of all three materials indicates that biosorption is not only a surface phenomenon but also that Pb^{2+} is able to penetrate into the peel particles. Since it is less practical to use the very small peel size (<0.6 mm), we used the peels 0.6–1.0 mm in size and allowed an equilibration time of 3 h for all further experiments.

The obtained equilibrium uptake of 0.7–0.9 mmol/g (1.4–1.8 mequiv./g) far exceeds the magnitude of charge observed in potentiometric titrations at pH 5 (Fig. 1) for protonated peels (0.33 mequiv./g) and original peels (0.01 mequiv./g), as used in the kinetic experiment. Apparently Pb^{2+} bound not only to free negatively charged sites but also replaced Ca^{2+} or H$^+$ from binding sites,

which may have included other sites with higher pK_a. The charge of carboxyl groups alone (0.33 mequiv./g), which should be mostly deprotonated at pH 5, cannot account for the magnitude of uptake. In isotherm studies (see below), higher metal concentrations were used, and consequently, the maximum capacity (2–3 mmol/g or 4–6 mequiv./g) was even higher than the uptake in the kinetic studies. Clearly, this high uptake could not have been achieved by electrostatic attraction to deprotonated carboxyl groups.

Comparison of different order models to Pb sorption data showed an inferiority of the first-order model for all three sizes of peels, with about twice as high RMSE values (Table 1, Fig. 4). The second- and third-order models generally provided similarly good predictions, with the third-order model having only slightly lower errors, except for the highest particle size, where it clearly fared best (Fig. 4). Ajmal et al. [10] found that Ni^{2+} biosorption by orange peels followed first-order kinetics, but did not consider higher-order models in their study. However, Reddad et al. [9] found that Ni^{2+} and Cu^{2+} biosorption by pectin-rich sugar beet pulp followed second-order kinetics. It is plausible that models b and d, where the rate is proportional to the square of the number of free sites, describe the kinetics of Pb^{2+} biosorption by orange peels. If a divalent ion like Pb^{2+} binds to two monovalent negatively charged surface sites, the rate should be proportional to the square of the remaining surface sites, which is the assumption of these models.
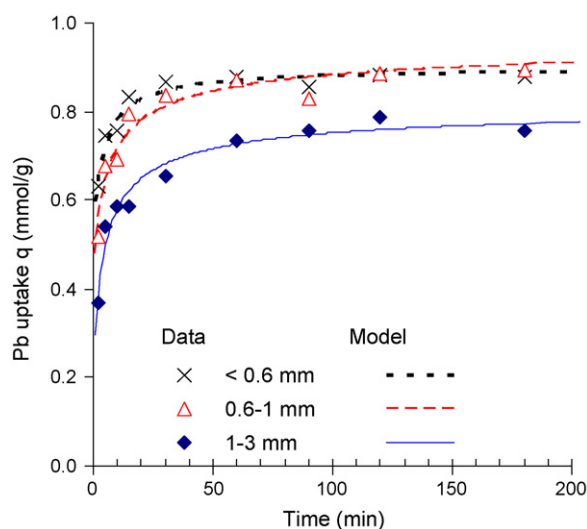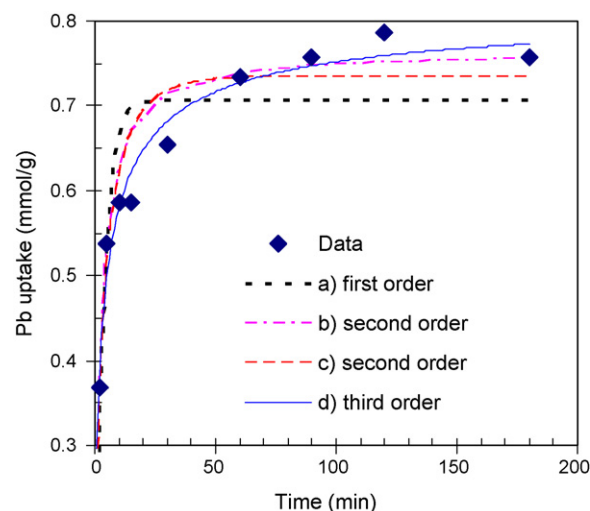
Fig. 3. Kinetics of Pb^{2+} binding by peels of different sizes and predictions of third-order model (pH 5, C_i 0.1 mM, S/L 0.1 g/L, 0.01 M NaNO$_3$).

Fig. 4. Kinetics of Pb^{2+} binding by peels of 1–3 mm and predictions of different models. (a) First-order model: rate proportional to number of free sites, $r = k(q_e - q)$; (b) second-order model: rate proportional to square of number of free sites, $r = k(q_e - q)^2$; (c) second-order model: rate proportional to Pb^{2+} concentration and number of free sites, $r = kC(q_e - q)$; (d) third-order model: rate proportional to Pb^{2+} concentration and square of number of free sites, $r = kC(q_e - q)^2$.
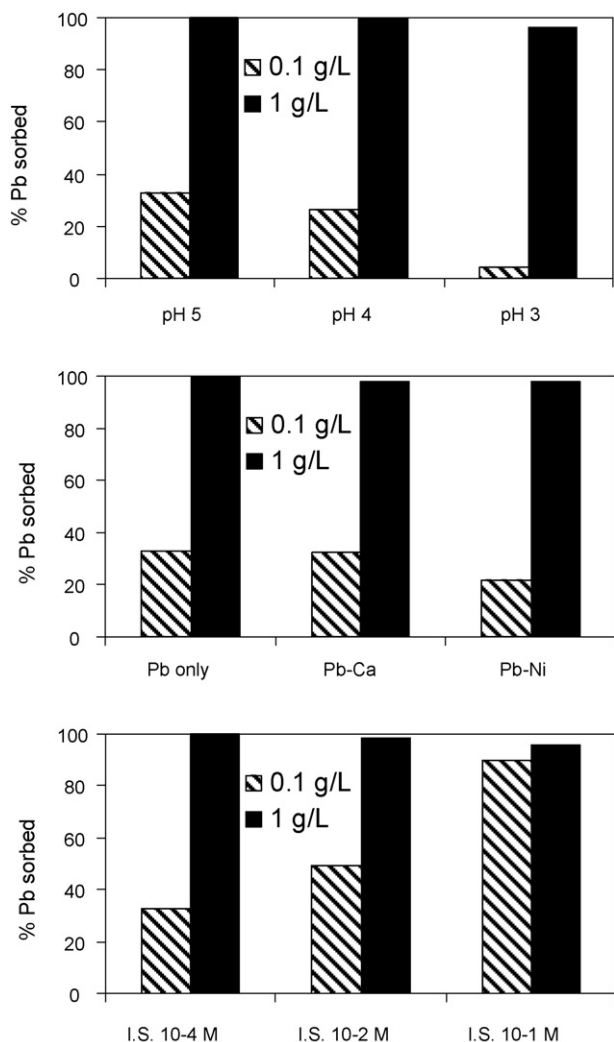
Fig. 5. Effect of process parameters on biosorption of 0.1 mM Pb^{2+} at pH 5 for peel dosages of 0.1 or 1 g/L. (a) Effect of pH, (b) effect of co-ions Ca and Ni, (c) effect of background electrolyte concentration (NaNO$_3$).

3.4. Effect of environmental conditions

The effect of different environmental conditions – pH, ionic strength, and competing ions – was studied for two different dosages of orange peels, representing limited and excess numbers of binding sites, respectively. Fig. 5a represents the effect of pH on biosorption by orange peels. The results show that a decrease in pH leads to a decreased removal of Pb^{2+} from the aqueous solution. This pattern was observed for both excess and limited surface sites. The pattern is analogous to the results of Annadurai et al. [15], who found an increase in metal ion uptake by banana and orange peels with increasing pH. The results can be attributed to the fact that at the higher pH values, more deprotonated negatively charged surface sites are available and competition by protons is lower, leading to higher metal uptake [34]. The results also show that when enough sorbent is available (1 g/L), effective removal of over 90% can be achieved even at pH 3, in contrast to the low sorbent dosage, where removal at pH 3 dropped to 4%, while removal at pH 5 was eight times higher.

The effects of competing ions Ca and Ni at equimolar concentrations on Pb^{2+} removal by orange peels can be observed in Fig. 5b. For excess surface sites, neither of the ions interfere much with Pb^{2+} sorption and only reduce Pb^{2+} removal by about 2%. For lim-

ited surface sites, Ca ions are still very weak competitors and do not interfere with Pb^{2+} biosorption whereas, Ni^{2+} ions decrease the lead removal by competing with Pb^{2+}. In comparison to that, Schiewer and Volesky [35] found for *Sargassum* biomass that at equimolar concentrations, coexisting Ca^{2+} reduced Cd^{2+} binding by about one-third, depending on the concentration level. However, when the Ca^{2+} concentration exceeds the Cd^{2+} concentration by a factor of 10, Cd^{2+} binding was drastically lowered in spite of a lower equilibrium binding constant for Ca^{2+} compared to Cd^{2+}.

Fig. 5c shows the effect of ionic strength on Pb^{2+} adsorption by orange peels. For excess sites, an increase in ionic strength slightly decreased sorption. These results are consistent with a study of Lee and Yang [5], who found a decrease in metal uptake by apple waste with ionic strength increase. For *Sargassum* algae, where carboxyl groups also constitute the main functional group, an even stronger effect of ionic strength on Cd biosorption was observed which was attributed to lowered intraparticle concentrations of Cd due to increased amounts of Na counter-ions in the vicinity of negatively charged sites [35]. The very slight effect of high ionic strength on biosorption of Pb^{2+} by citrus peels indicates that electrostatic attraction is not the main binding mechanism, but that stronger chemical bonds not affected by high Na concentrations must exist.

When the sites were limited, an unusual observation was made: increased ionic strength increased the overall removal. A theoretical metal speciation study for a solution with 0.1 mM Pb^{2+} in an open system revealed that if no NaNO$_3$ was added, virtually all Pb was present as Pb^{2+}, and at 0.01 M NaNO$_3$, over 90% of Pb still occurred as Pb^{2+}. At 0.1 M NaNO$_3$, however, only 62% occurred as Pb^{2+}, while 34% occurred as PbNO$_3^+$. This change in speciation may have been responsible for increased binding at these conditions. It is possible that total Pb binding increases because each PbNO$_3^+$ ion only requires one binding site compared to two sites per Pb^{2+}.

3.5. Biosorption isotherm

The metal uptake as a function of the equilibrium concentration of Pb is presented in Fig. 6. The data show increased uptake with increasing concentration whereby the slope of the curve gradually decreased. The most common biosorption models representing this phenomenon are the Langmuir and Freundlich models. Langmuir and Freundlich parameters were obtained both by linear and nonlinear fitting and tabulated in Table 2. Though Freundlich isotherms had lower RMSE, no solid conclusions about the appropriateness of Langmuir versus Freundlich isotherms can be drawn since the experiment had to be confined to relatively low concentrations where no site saturation was reached. Predictions of both models with nonlinear parameter optimization are shown in Fig. 6. Even
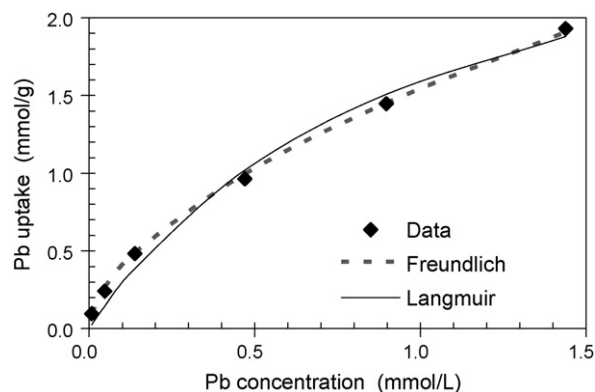

Fig. 6. Biosorption isotherm for Pb^{2+} binding by orange peels (size 0.6–1.0 mm) at pH 5. Data and Langmuir model with nonlinear parameter optimization.

Table 2
Equilibrium parameters for Langmuir and Freundlich isotherm models

Isotherm	Type	Model parameter		R^2	RMSE
Langmuir	Linear	$K = 2.3$ L/mmol	$q_{max} = 2.32$ mmol/g	0.913	0.130
	Nonlinear	$K = 1.0$ L/mmol	$q_{max} = 3.18$ mmol/g	n/a	0.073
Freundlich	Linear	$k_f = 1.52$ $L^{0.58}$ g^{-1} $mmol^{0.42}$	$n = 1.72$	0.999	0.024
	Nonlinear	$k_f = 1.54$ $L^{0.58}$ g^{-1} $mmol^{0.42}$	$n = 1.72$	n/a	0.018

though nonlinear parameter determination requires a little more computational effort, it should be used because of the better fit, as apparent from the RMSE values in Table 2.

The Pb uptake of ~2 mmol/g (~400 mg/g) observed for citrus peels in this study were very high: citrus peels can accumulate almost half their weight in Pb. This capacity is similar to that of synthetic cation exchange resins. The biosorption capacity was higher than that expected based on potentiometric titrations, indicating that attraction by negatively charged groups is not the only governing mechanism. Pb^{2+} ions might be replacing protons as well as Ca^{2+} or other naturally present ions in the original orange peels. It should be noted that at the experimental conditions, the maximum uptake capacity was not yet reached. This means metal uptake could be even higher: the extrapolated maximum capacity according to the Langmuir model was 3.18 mmol/g (658 mg/g). This value is however only an estimate, not experimentally confirmed.

3.6. pH variability during adsorption

As the result of an incremental addition of Pb^{2+} to a suspension of original unprotonated peels, the pH decreased as shown in Fig. 7. This can be explained by successive replacement of protons from functional groups by increasing amounts of divalent Pb^{2+} ions. This phenomenon occurred not only for orange peels but also for HM and LM pectins [21]. The cumulative proton release was highest for LM pectin, which contained the highest number of carboxyl groups (degree of methoxylation ~9%) and proton release was lowest for orange peels, which is consistent with a lower overall number of functional groups, as also evident from the low surface charge observed in potentiometric titration. In general, the results show that acidic functional groups are involved in Pb^{2+} biosorption and undergo acid–base reactions between pH 4 and 5. The number of protons released during Pb^{2+} binding, however, is low compared to the metal uptake. Apparently exchange between protons and Pb^{2+} played a minor role

because under the experimental conditions, most groups were already deprotonated or saturated with other ions such as Ca^{2+}.

4. Conclusions

As shown in FTIR studies, citrus pectin and peels have similar surface functional groups whereby carboxylic acid groups of pectin are involved in Pb^{2+} binding. Biosorption of Pb^{2+} by orange peels is fast, with equilibrium reached in 30–90 min, and follows second- or third-order kinetics. Nonlinear parameter optimization for isotherms and kinetic models provided a better fit than linearizations.

Pb^{2+} uptake by orange peels depends on pH, ionic strength, and presence of co-ions, but at high sorbent dosage, these parameters had little impact and Pb^{2+} removal remained >90%. The proton release during Pb^{2+} binding could not account for the amount of Pb^{2+} taken up, indicating that Pb^{2+} bound mainly to sites not occupied by protons. The negative charge of the sorbent was low compared to the binding capacity, indicating that electrostatic attraction could not be a primary binding mechanism. This finding was also supported by the observation that strong increases in ionic strength did not reduce Pb^{2+} binding significantly. To the contrary, Pb^{2+} binding even increased with increasing ionic strength for low sorbent dosages.

The highest measured Pb^{2+} uptake by orange peels was 1.93 mmol/g, which corresponds to approximately 400 mg/g. However, no plateau value was reached for that concentration. The maximum uptake capacity according to the Langmuir model was 3.18 mmol/g or 658 mg/g, which is very high for biosorbents and similar to some ion exchange resins.

Overall, this study suggests that biosorption of Pb^{2+} ions by orange peels can be an inexpensive and effective way of metal ion treatment and should be investigated further for its practical application.

Fig. 7. pH variability and proton release (delta H) by citrus pectin and protonated peels for incremental addition of Pb^{2+} up to 0.1 mM.

References

[1] B. Volesky, Biosorption of Heavy Metals, CRC Press Inc., Boca Raton, USA, 1990.
[2] T.A. Davis, B. Volesky, M. Alfonso, A review of the biochemistry of heavy metal biosorption by brown algae, Water Res. 37 (2003) 4311–4330.
[3] G.T. Grant, E.R. Morris, D.A. Rees, P.J.C. Smith, D. Thom, Biological interactions between polysaccharides and divalent cations: the egg-box model, FEBS Lett. 32 (1973) 195–198.
[4] R. Kohn, Binding of divalent cations to oligomeric fragments of pectin, Carbohyd. Res. 160 (1987) 343–353.
[5] S.H. Lee, J.-W. Yang, Removal of copper in aqueous solution by apple waste, Sep. Sci. Technol. 32 (8) (1997) 1371–1387.
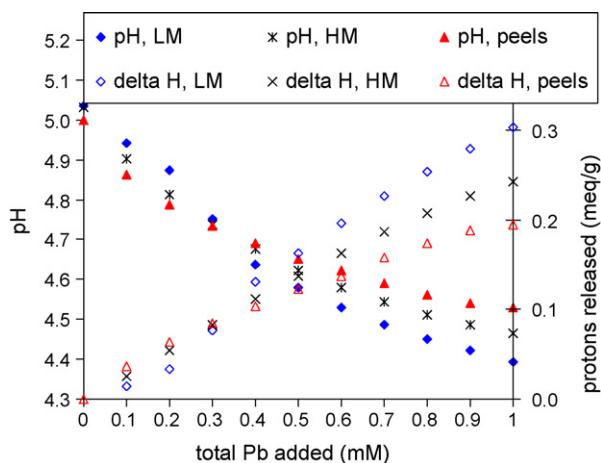
[6] E. Maranon, H. Sastre, Behavior of lignocellulosic apple residues in the sorption of trace metals in packed beds, React. Polym. 18 (1992) 173–176.

[7] V.M. Dronnet, C.M.G.C. Renard, M.A.V. Axelos, J.F. Thibault, Characterization and selectivity of divalent metal ion binding by citrus and sugar beet pectin, Carbohyd. Polym. 30 (1996) 253–263.

[8] C. Gerente, P.C. du Mesnil, Y. Andres, J.F. Thibault, P. Le Cloirec, Removal of metal ions from aqueous solution on low cost natural polysaccharides. Sorption mechanism approach, React. Funct. Polym. 46 (2) (2000) 35–144.

[9] Z. Reddad, C. Gerente, Y. Andres, P. Le Cloirec, Modeling of single and competitive metal adsorption onto a natural polysaccharide, Environ. Sci. Technol. 36 (10) (2002) 2242–2248.

[10] M. Ajmal, R.A. Khan-Rao, R. Ahmad, J. Ahmad, Adsorption studies of *Citrus reticulata* (fruit peel of orange): removal of Ni(II) from electroplating wastewater, J. Hazard. Mater. 79 (1–2) (2000) 117–131.

[11] K. Inoue, K.N. Ghimire, Y. Zhu, M. Yano, K. Makino, T. Miyajima, Effective use of orange juice residue for removing heavy and radioactive metals from environments, Geosyst. Eng. 5 (2) (2002) 31–37.

[12] X. Li, Y. Tang, Z. Xuan, Y. Liu, F. Luo, Study on the preparation of orange peel cellulose adsorbents and biosorption of Cd from aqueous solution, Sep. Purif. Technol. 55 (1) (2007) 69–75.

[13] A.B. Perez-Marin, V. Meseguer Zapata, J.F. Ortuno, M. Aguilar, J. Saez, M. Llorens, Removal of cadmium from aqueous solutions by adsorption onto orange waste, J. Hazard. Mater. B139 (2007) 122–131.

[14] S. Senthilkumaar, S. Bharathi, D. Nithyanandhi, V. Subburam, Biosorption of toxic heavy metals from aqueous solutions, Bioresour. Technol. 75 (2) (2000) 163–165.

[15] G. Annadurai, R.S. Juang, D.J. Lee, Adsorption of heavy metals from water using banana and orange peels, Water Sci. Technol. 47 (2003) 185–190.

[16] R. Jumle, M.L. Narwade, U. Wasnik, Studies in adsorption of some toxic metal ions on *Citrus sinesis* skin and *Coffea arabica* husk: Agricultural by product, Asian J. Chem. 14 (2002) 1257–1260.

[17] S. Schiewer, S.B. Patil, Pectin-rich fruit wastes as biosorbents for heavy metal removal: equilibrium and kinetics, Bioresour Technol. 99 (6) (2008) 1896–1903.

[18] W. Stumm, J.J. Morgan, Aquatic Chemistry, Wiley–Interscience, A Division of John Wiley & Sons, Inc., New York, 1970.

[19] S. Schiewer, B. Volesky, Ionic strength and electrostatic effects in biosorption of protons, Environ. Sci. Technol. 31 (1997) 1863–1871.

[20] S. Schiewer, S.B. Patil, Modeling the effect of pH on biosorption of heavy metals by citrus peels, J. Hazard. Mater. 157 (2008) 8–17.

[21] A. Balaria, S. Schiewer, Assessment of biosorption mechanism for Pb binding by citrus pectin, Sep. Purif. Technol., in press.

[22] R. Gnanasambandam, A. Proctor, Determination of pectin degree of esterification by diffuse reflectance Fourier transform infrared spectroscopy, Food Chem. 68 (3) (1999) 327–332.

[23] M.A. Monsoor, U. Kalapathy, A. Proctor, Improved method for determination of pectin degree of esterification by diffuse reflectance Fourier transform infrared spectroscopy, J. Agric. Food Chem. 49 (6) (2001) 2756–2760.

[24] Y.S. Ho, J.C.Y. Ng, G. McKay, Kinetics of pollutant sorption by biosorbents: a review, Sep. Purif. Methods 29 (2) (2000) 189–232.

[25] Z. Xuan, Y. Tang, X. Li, Y. Liu, F. Luo, Study on the equilibrium, kinetics and isotherm of biosorption of lead ions onto pretreated chemically modified orange peel, Biochem. Eng. J. 31 (2006) 160–164.

[26] R. Juang, M. Chen, Application of the Elovich equation to the kinetics of metal sorption with solvent-impregnated resins, Ind. Eng. Chem. Res. 36 (1997) 813–820.

[27] S. Lagergren, About the theory of so-called adsorption of soluble substances, K. Sven. Vetenskapsakad. Handl. 24 (1898) 1–39.

[28] Y.S. Ho, G. McKay, The kinetics of sorption of basic dyes from aqueous solution by sphagnum moss peat, Can. J. Chem. Eng. 76 (1998) 822–827.

[29] J. Buffle, Complexation of Reactions in Aquatic Systems—An Analytical Approach, Ellis Horward Limited, Chichester, UK, 1988.

[30] E. Fourest, B. Volesky, Contribution of sulphonate groups and alginate to heavy metal biosorption by the dry biomass of *Sargassum fluitans*, Environ. Sci. Technol. 30 (1996) 277–282.

[31] C. Jeon, J.Y. Park, Y.G. Yoo, Biosorption model for binary adsorption sites, J. Microbiol. Biotechnol. 11 (2001) 781–787.

[32] Y. Murphy, H. Hughes, P. McLoughlin, Cu(II) binding by dried biomass of red, green and brown macroalgae, Water Res. 41 (2007) 731–740.

[33] Y.S. Yun, D. Park, B. Volesky, Biosorption of trivalent chromium on the brown seaweed biomass, Environ. Sci. Technol. 35 (2001) 4353–4358.

[34] S. Schiewer, B. Volesky, Modeling of the proton–metal ion exchange in biosorption, Environ. Sci. Technol. 29 (1995) 3049–3058.

[35] S. Schiewer, B. Volesky, Ionic strength and electrostatic effects in biosorption of divalent metal ions and protons, Environ. Sci. Technol. 31 (1997) 2478–2485.